A BVR_CI_C Survey of W Ursae Majoris Binaries

Dirk Terrell

Department of Space Studies, Southwest Research Institute, 1050 Walnut St., Suite 300, Boulder, CO 80302

terrell@boulder.swri.edu

John Gross

Sonoita Research Observatory, 1442 E Roger Rd, Tucson, 85719

johngross3@msn.com

and

Walter R. Cooney, Jr.

Lot No. 23, Palanamai Village, 281 Burapha Golf Club, Moo 4, Bung, Sriracha, Chonburi 20110 Thailand

waltc@cox.net

ABSTRACT

We report on a BVR_CI_C survey of field W Ursae Majoris binary stars and present accurate colors for 606 systems that have been observed on at least three photometric nights from a robotic observatory in southern Arizona. Comparison with earlier photometry for a subset of the systems shows good agreement. We investigate two independent methods of determining the interstellar reddening, although both have limitations that can render them less effective than desired. A subset of 101 systems shows good agreement between the two reddening methods.

Subject headings: binaries: close — binaries: eclipsing

1. Introduction

Overcontact binary stars[1] are systems in which both components share a common envelope between the inner and outer contact surfaces, and are therefore in physical contact with one another, leading to luminosity and mass exchange. Such systems show light curves with very similar eclipse depths and little color variation over the orbital cycle. The W Ursae Majoris systems are the most well-known overcontact systems, consisting of F, G and K-type stars with convective common envelopes. But early-type systems with radiative common envelopes do exist (Terrell, et al. 2003) and are even quite common among the O-type stars (Hilditch & Bell 1987).

Despite over four decades of efforts to understand their internal structure and evolution, no model has emerged as clearly superior in explaining their observed properties, although active work (e.g., Stępień (2009) and Stępień (2011)) does show promise. Almost all of the theoretical work on overcontact systems has involved the W UMa systems, although the evolutionary models of Nelson & Eggleton (2001) show that the overcontact state is achieved for a wide variety of binary initial conditions (*viz.* their Figure 9). The seminal work by Lucy (1968) showed that overcontact systems with common convective envelopes could exist at zero-age but the agreement of his models with the observed period-color relation (Eggen 1967) was not very good and Eggen's period-color relation has played a critical role in the testing of models of W UMa systems ever since. The primary goal of this survey is to provide a significantly larger sample of

---

[1]We note that there is a preference among some in the community for the term "contact" rather than "overcontact." Rucinski (1997a) and Wilson (2001) discuss both sides of the issue.

overcontact systems with accurate photometry and to extend the photometry to the $R_C I_C$ passbands.

Although the proliferation of relatively inexpensive CCD cameras and telescopes has resulted in a large body of light curve data for W UMa systems, most of these data are instrumental differential magnitudes rather than transformed standard magnitudes, a circumstance dictated in most cases by the predominantly non-photometric skies available to the observers. Rucinski (2006) discusses the period-color-luminosity relationship for W UMa systems and its use as a distance indicator for these systems. One goal of our program is to provide more accurate color data than is currently available for this calibration. Accurate colors are also necessary for light curve solutions where the spectral type of the system is not available.

2. Sonoita Research Observatory

2.1. Hardware

The goal of our survey program is to measure accurate colors of a large number of W UMa systems brighter than 14th magnitude visible from our observatory in Sonoita, Arizona. The equipment at the Sonoita Research Observatory (SRO) consists of a 0.35m Schmidt-Cassegrain telescope on a robotic German equatorial mount, a Santa Barbara Instrument Group STL-1001E CCD camera and a Custom Scientific $BVR_C I_C$ filter set with the Bessell (1990) prescriptions. With this equipment, we can achieve photometric precisions of 0.01 magnitudes at 14th magnitude with reasonable integration times.

The observatory sits on a private site located about 60 miles east-southeast of Kitt Peak National Observatory in very dark skies. Previously unknown main-belt asteroids in the 19th-20th magnitude range have been discovered in five-minute unfiltered images taken at SRO, and stacked, unfiltered images have revealed 23rd magnitude stars. Seeing is typically $2''$-$3''$ full-width at half maximum.

2.2. Software

As with all robotic observatories, the main determinant of observing efficiency at SRO has been the software used to control the telescope and camera. All of the observing software we use is commercially available. The two key software programs are ACP Observatory Control Software (hereafter, ACP) and ACP Scheduler from DC-3 Dreams, Incorporated of Mesa,

Arizona.[2] Overall operations control is handled by ACP. At the beginning of each night, it opens the dome, and takes twilight flats. During the night, it monitors the weather conditions (closing the dome if the weather degrades to a dangerous state), moves the telescope and dome, instructs the camera control software to take images, and monitors the telescope focus, refocusing as needed. At the end of the night, it takes more twilight flats and then parks the telescope and closes the dome. The entire operation is run unattended, allowing for a tremendous increase in observing efficiency over traditional human-driven telescope operations.

The primary enabler of a survey project like this one is the scheduling software. The ACP Scheduler is a real-time scheduler that can adjust to changing observing conditions and observing priorities, as opposed to the traditional queue schedulers that decide the observing plan at the beginning of the night. Executing a survey like this one involves merely entering the coordinates of the desired fields (i.e. standard star fields and the object fields), filters and exposure times into the ACP Scheduler database once. At the start of each night, the scheduler chooses the best field to observe. When that field is completed, a new field is chosen based on the current conditions. If the weather degrades from photometric conditions, but is still reasonable for differential photometry projects, the scheduler will begin doing those. Should the weather later improve, it will return to projects like the survey that require photometric skies. The scheduler thus makes the most efficient use of the observing time, all without human intervention.

3. Data Gathering and Processing

While the observatory operation for the survey is untraditional, the data gathering is not. The goal is to measure the program stars in four Johnson-Cousins filters ($BVR_C I_C$) and transform the observations to the standard system via the observation of Landolt (1983, 1992) standard fields. Our approach is to separate the determination of the extinction coefficients from the transformation coefficients. We observe a reasonably bright star with a $B - V$ value near zero through each filter periodically during the night as it moves through a reasonable range of airmass, typically from 1.0 to 2.5 airmasses. The star is chosen so that it can be observed low in the eastern sky at the beginning of the night, up

---

[2]Web site at `http://www.dc3.com`

2

to the zenith, and then in the western sky late in the night. This approach typically yields about a dozen measurements through each filter per night, and covers both sides of the meridian, providing a diagnostic of the photometric quality of the night. A linear fit of instrumental magnitude versus airmass then provides the (first-order) extinction coefficient.

Observations of standard and target fields are made in the sequence I_C, R_C, V, B, and then B, V, R_C, I_C to minimize extinction issues. The two magnitude measurements for each star in each filter are averaged to provide coeval values for forming colors. Determination of the transformation coefficients is done in the usual way by observing several Landolt standard fields near the meridian during the night and then performing linear fits to the various instrumental versus standard magnitude plots.

As images are collected during the night, they are losslessly compressed and transferred to a storage server at the lead author's institution. Processing of the images is performed with scripts written in PyRAF, a Python interface to IRAF available from the Space Science Institute web site.[3] They are then bias and dark subtracted and flatfielded. Extinction coefficients are first determined and then the transformation coefficients determined. This part of the process is interactive, with plots that allow the user to determine the quality of the night and delete obviously bad images from the reduction. Once the extinction and transformation coefficients are known, the images of target fields can be reduced and the observations transformed onto the standard system. Aperture photometry is performed with an aperture radius of eight pixels, sky annulus radius of twelve pixels and an annulus thickness of three pixels. The pixels subtend $1''.24$ on the sky.

4. Survey Targets and Results

The survey began in 2005 with targets selected from the Pribulla, Kreiner, & Tremko (2003), hereafter PKT, catalog of 361 overcontact systems. Soon thereafter, Gettel, Geske, & McKay (2006), hereafter GGM, published a catalog of 1022 overcontact systems identified from ROTSE-I sky patrol images. The final list of observed targets came primarily from these two catalogs, with two systems (GSC 0067-00348 and

GSC 2545-00970) added after we made follow-up observations of new discoveries. The last of the observations reported herein were made in 2008. Observations were made on 237 photometric nights, with this project sharing telescope time with several other survey projects.

In total, 606 systems with $9 \leq V_{max} \leq 13$ had observations of sufficient quality to be listed in Table 1. The table is given in abbreviated form in the printed version of the paper to show the file structure, with the full table given in the online version. The star identifications are either the GCVS designation, if known, or the designation given in GGM. The objects listed by their indentification from the GGM catalog can be searched in the SIMBAD database by using the "ggm2006" catalog identifier. We chose to retain the GGM designation because SIMBAD does not list Guide Star Catalog identifications of many of these systems. The positions, orbital periods and maximum/minimum V magnitudes are taken from either the PKT or the GGM catalogs. In a handful of cases, the positions are from astrometry of our images where the GGM positions were ambiguous due to blending. All systems were observed on at least three nights but 251 systems had observations on four or more nights. The $B - V$, $V - R_C$, and $R_C - I_C$ colors are given as measured, and the $V - I_C$ color is formed as the sum of $V - R_C$ and $R_C - I_C$. The errors given are the standard deviations of the individual measurements, and this include both the measurement errors and any intrinsic color changes in the stars, which we assume to be small.

To assess the accuracy of the colors, they were compared to values found in the Tycho catalog and from other sources in the literature. The bulk of the comparison data came from the Tycho catalog and were selected for comparison to our data if the error listed in the Tycho catalog was 0.05 mag or less. To extend the comparison past $B - V = 1$, values for CC Com (Bradstreet 1985), VZ Psc (Bradstreet 1985), and V523 Cas (Samec, Faulkner, & Williams 2004) were taken from the literature. Figure 1 shows our $B - V$ values plotted against the comparison data. Figure 2 shows our $V - I_C$ values plotted against values from Tycho and the literature. Once again, the red end of the figure was extended past the range of accurate Tycho values, with the value for XY Leo taken from Hrivnak (1985) and values for CC Com, VZ Psc, V523 Cas, V574 Lyr, CT Tau, LR Cam, 766402, 7710246, and 13149917 taken from The Amateur Sky Survey Mark IV (TASS) (Droege, et al. 2006). On the blue end, values for CT

Tau and 2962451 were also taken from the TASS catalog. Both figures show good agreement between our photometry and that of others.

We examined our data for any systematic dependences of the errors on various quantities. One obvious dependence would be on the magnitude of the binary. In a constant-exposure survey, this type of dependence is expected and easily revealed. Our survey, however, had exposures optimized for each individual system, and our targets are all in the brightness range where we expect intrinsic color variability and the transformation to the standard system to be the dominant noise sources, rather than sources like photon noise or sky background noise. In that case, we do not expect to see any strong dependence on the brightness of the system and Figure 3 shows this to be the case.

Another possibility is a dependence of the color error on the color itself. Our exposure times were determined using the V magnitude of the binary at maximum brightness and the known sensitivity of the equipment for each filter. Redder systems would require a longer exposure in B than a bluer system of the same brightness in order to have the same signal-to-noise ratio for photon noise (the dominant noise source in a given exposure for our equipment and the magnitude range of our survey). Since our exposures were set to achieve a signal-to-noise ratio of 200 or better (for photon noise) for each exposure, we still expect the observed errors to be dominated by intrinsic variablity and transformation uncertainties. Figure 4 shows that this is indeed the case.

5. Reddening

To be of the most usefulness, the colors of the stars need to be corrected for the effect of interstellar reddening. Normally, an accurate measurement of the reddening requires a detailed spectroscopic analysis, such as that employed by Terrell, et al. (2003) using the Na D lines as calibrated by Munari & Zwitter (1997). For the majority of the systems in our survey, such data do not exist. We therefore present a preliminary analysis using two approaches for which complete data are available: determining a reddening-free quantity from our photometry, and computing the reddening from the neutral hydrogen column density, N_{HI}, along the line of sight to the system. The former approach, referred to hereafter as the color difference method, follows that used for early-type stars with $U - B$ and $B - V$ colors to determine the reddening-
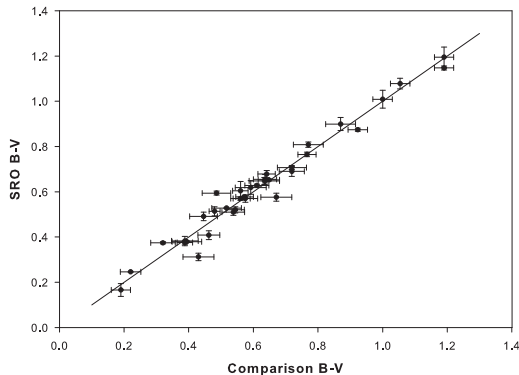

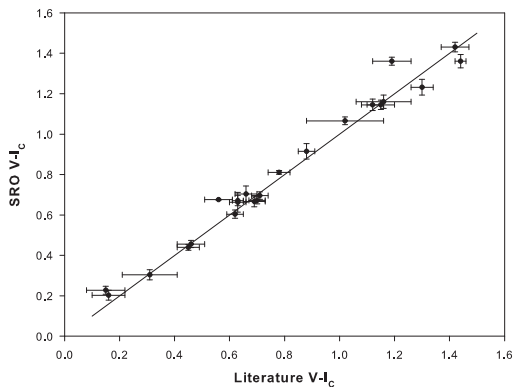Fig. 1.— SRO $B - V$ values compared to $B - V$ values in the literature for 35 systems.

Fig. 2.— SRO $V - I_C$ values compared to $V - I_C$ values in the literature for 23 systems.
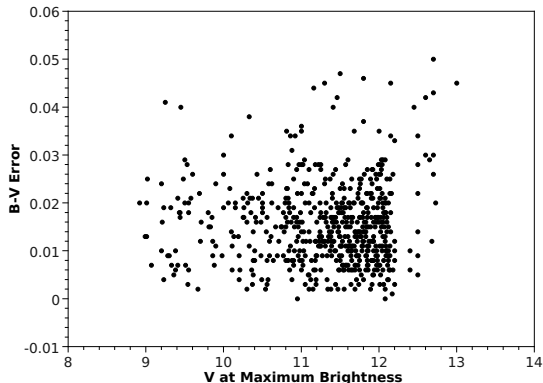
4

Fig. 3.— The error in $B - V$ versus the V magnitude for all systems in the survey.
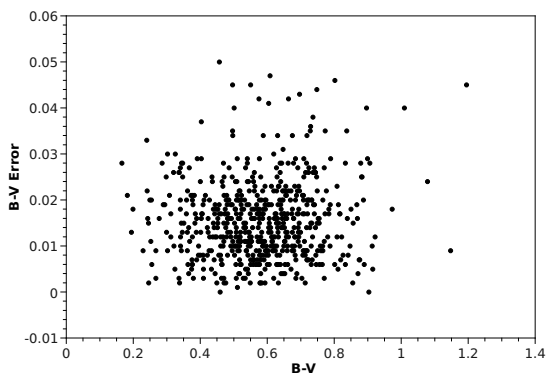

Fig. 4.— The error in $B - V$ versus $B - V$ for all systems in the survey.

free parameter Q (Johnson & Morgan 1953). The latter is the method employed by Rucinski (1997) in calibrating the absolute magnitudes of W UMa systems. While these approaches have limitations, as discussed below, we believe they can provide useful information until better data can be obtained.

Following conventional notation, we write the observed color as $B - V$, the unreddened color as $(B - V)_0$, and the reddening as $E(B - V)$ so that $B - V = (B - V)_0 + E(B - V)$. The color difference method uses the difference in two colors to form a reddening-free quantity usually respresented by the letter Q. The key is to mutiply one of the colors by a constant factor representing the ratio of the color excesses for the two colors, $i.e.$, $Q = C1 - \frac{(E(C1)}{E(C2)} \times C2$. While the traditional Q quantity, $(U - B) - \frac{E(U-B)}{E(B-V)} \times (B - V)$, is not useful for the stars of spectral types in this survey, the basic idea can be applied to more appropriate filters. Here we use the $B - V$ and $V - I_C$ colors, and thus define Q as $(B - V) - \frac{E(B-V)}{E(V-I_C)} \times (V - I_C)$. Using the absorption ratios, $\frac{A(\lambda)}{A(V)}$, given in Cardelli, Clayton, & Mathis (1989) and assuming a total to selective extinction ratio of $R_V = 3.1$, the ratio $\frac{E(B-V)}{E(V-I)}$ has a value of 0.647.

Figure 5 is the color difference diagram for all of the systems in the survey. The solid curve shows the main sequence from Walker (1985) for $V - I_C \leq 0.95$ and Cousins (1978) for $V - I_C > 0.95$. Because Q is reddening-independent, the reddening lines in such a diagram are horizontal and can be used to estimate the reddening of a given star. The horizontal line in Figure 5 shows the reddening of a main sequence star with $(V - I_C)_0 = 0.79$ and the vertical ticks indicate increasing reddening in steps of 0.1 in $E(B - V)$.

One concern with this approach to determining the reddening is that many, perhaps all (Pribulla & Rucinski 2008), of these objects have companions and this can have a large effect on the color difference diagram. If, as is usually the case, the companions are cool, low-mass objects, they will affect the longer wavelength filters more than the shorter ones, and make the systems look redder than they otherwise would be. However, except in most circumstances, we expect the third bodies to be of low luminosities, making the effect on the system colors fairly small, perhaps a few hundredths of a magnitude. Unfortunately, these errors are large enough to greatly diminish the usefulness of the color difference diagram for systems only slightly af-
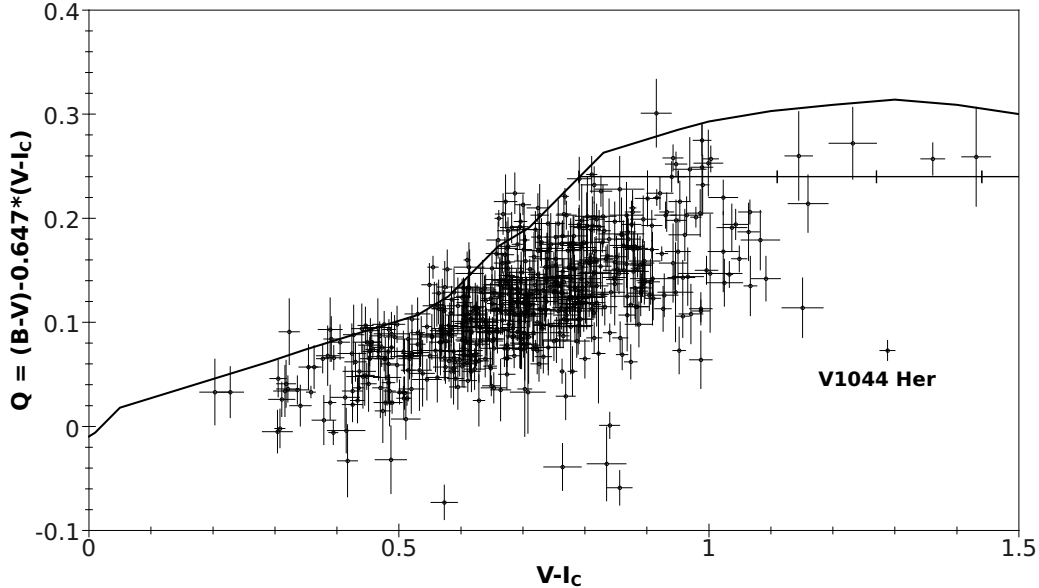
5

Fig. 5.— Q versus $V - I_C$ for the stars in the survey. The solid curve is the zero-age main sequence from Walker (1985) and the horizontal line is a reddening line for a star with $(V - I_C)_0 = 0.79$ with the ticks representing steps of 0.1 in $E(B-V)$.

fected by interstellar reddening, as we expect most of these systems to be due to their brightnesses, and thus nearby distances.

While not as useful as we had hoped for determining reddening, the color difference diagram does distinguish a few systems as being unusual. Figure 5 shows a few systems at large horizontal distances from the main sequence curve, such as V1044 Her whose $E(V - I_C)$ value from the color difference diagram is about 0.9. The question is whether that is caused by large interstellar reddening, or something else, such as a luminous companion. Looking at the expected reddening from the neutral hydrogen column density provides a clue.

Predehl & Schmitt (1995) used ROSAT observations to determine the relationship between X-ray absorption and optical extinction. Again assuming $R_V = 3.1$, their results show that $E(B-V) = 1.8 \times 10^{-22} \times N_{HI}$. To compute the N_{HI} value for individual systems, we used the "nh" tool in the "heasarc" sub-package of the FTOOLS software available from the NASA Goddard Spaceflight Center.[4] Although this

approach to estimating the reddening doesn't suffer the same problems as the color difference method, it does have potential problems. The main issue is that the N_{HI} column density is estimated by interpolating between the approximately 0.5 degree sampling points of the N_{HI} surveys as described in the software documentation. Caution must be exercised in using this method in areas where there are inhomogeneities in the interstellar medium on the scale of the interpolation. With that caveat in mind, we can compute the reddening and compare it to the value from the color difference method.

In the case of V1044 Her, we find that the value of $E(B-V)$ from estimated from the N_{HI} column density is 0.05, while $E(B-V)$ from the color difference method is 0.58. In order for the color difference value to be correct, the system would have to have a $(B-V)_0$ value of about 0.34, making it an early F-type star, but its orbital period of about 0.24 days precludes a spectral type that early. In this case, the reddening estimate based on the N_{HI} column density seems much more reasonable, but that leaves unanswered the question of why the $B - V$ value, implying $T_{eff} \approx 5000K$, and the $V - I_C$ value, implying $T_{eff} \approx 4300K$, are so disparate. The $V - R_C$ and $R - I_C$ values, 0.69 and 0.60 respec-

---

[4]Available at http://heasarc.gsfc.nasa.gov/lheasoft/ftools/heasarc.html

tively, are consistent with the $V - I_C$ value, implying that the $B - V$ value is too blue. The system was measured on three nights within a week of one another, and the three $B - V$ values were consistent with one another, with values of 0.91, 0.92 and 0.92. The images show no obvious problems and the unfiltered light curve of Blattler & Diethelm (2001) does not appear to have large amounts of third light, so the reason for the disparity remains unclear. Perhaps the system is more active than usual, leading to elevated brightness in the B filter. Being one of only a few known systems with an orbital period less than 0.25 days, further observational study of V1044 Her is warranted.

The N_{HI} method occasionally produces reddening values that are very large compared to the color difference method. One example is V1191 Cyg whose $E(B-V)$ from the color difference method is 0.05 while the N_{HI} method yields a value of 1.13. This difference is not very surprising since Cygnus lies along the galactic plane and large inhomogeneities in the interstellar medium are to be expected. Because of the weaknesses of each method, the safest approach is to trust only reddening values where the two methods are in good agreement. There are 321 systems that have equal values within the error bars, with the error in the N_{HI} method assumed to be 0.02 magnitudes. However, of those, many have fairly large errors in the values from the color difference method, with many having errors significantly larger than the value itself. To generate a more useful list, we further culled the list by eliminating systems where the difference between the two methods was 0.02 mag or less. This culling leaves 101 systems where the reddening values between the two methods are consistent. Table 2 shows how the values compare for these 101 systems.

Figure 6 shows the period-color relation for the systems in Table 2 along with the systems from Rucinski (1997) with periods less than 0.6 days. The solid line is the short period blue envelope (SPBE) from Rucinski (1998) which can be likened to the zero-age main sequence for overcontact binaries in that systems will evolve towards redder colors and longer periods. Overcontact systems are thus not expected to be bluer than the SPBE. The systems in Figure 6 that are bluer than the SPBE by more than one standard deviation in the $B - V$ value (3091792, 6133549, 3947987, 2569021, 9649548, 3962973, 8299111, 6225358, and V523 Cas) could be systems that are not overcontact systems, systems with a blue companion or they may be systems where our estimate of the reddening is too

large. In the case of V523 Cas (whose overcontact nature appears solidly established), Samec, Faulkner, & Williams (2004) find $B - V = 1.03$ to 1.09 for the binary and $(B - V)_0 = 0.97 \pm 0.04$ for the primary component, whereas we find $B - V = 1.08 \pm 0.02$ and $(B - V)_0 = 0.89 \pm 0.03$ for the binary. Their analysis of the O-C digram results in a third body mass of about $0.4 M_\odot$, which would not explain the "blue excess" of the system, and since there is good agreement between their reddened $B - V$ and ours, the difference may lie in the determination of the reddening, or perhaps intrinsic activity in the system that enhanced the brightness in the B filter during our observations. We note that both the color difference and the N_{HI} methods show good agreement for the reddening in V523 Cas (see Table 2). Further observational studies of these systems will be needed to determine their nature.

6. Conclusions

Standardized photometry in Johnson-Cousins BVR_CI_C filters was obtained for 606 known or suspected W UMa eclipsing binaries. Gettel, Geske, & McKay (2006), from which a large fraction of the targets in this survey were taken, estimate that perhaps 5% of the systems in their catalog may be objects other than W UMa systems, so we have a reasonably pure sample of such binaries. Comparison of our results with previously published photometry on a few dozen systems shows good agreement. Estimates of the interstellar reddening were made with the color difference method and by using the neutral hydrogen column density along the line of sight to the stars. While neither approach is ideal, they each have strengths and are based on independent observational data. A subset of 101 systems in the survey shows good agreement between the two methods. It is hoped that these data will be useful in further research to understand the nature of these very interesting binaries.

REFERENCES

Bessell, M.S. 1990, PASP, 102, 1181

Blattler, E. & Diethelm, R. 2001, Inf. Bull. Variable Stars, No. 5192

TABLE 1

THE BVR_CI_C COLORS OF 606 W URSAE MAJORIS BINARIES.

System	R.A. (° J2000)	Decl. (° J2000)	Period (days)	Num. Obs.	$B-V$	$V-R_C$	R_C-I_C	$V-I_C$	V_{max}	V_{min}
299755	1.4917	78.9081	0.43821290	3	0.562 ± 0.016	0.332 ± 0.003	0.348 ± 0.004	0.680 ± 0.005	11.83	12.50
1557554	1.6542	55.4561	0.27249130	3	0.874 ± 0.007	0.510 ± 0.007	0.432 ± 0.016	0.942 ± 0.017	9.33	9.64
V1007 Cas	2.0125	51.1342	0.33201060	3	0.724 ± 0.027	0.459 ± 0.004	0.437 ± 0.010	0.896 ± 0.011	12.03	12.43
11936075	3.9833	6.7457	0.40117920	3	0.519 ± 0.012	0.308 ± 0.008	0.332 ± 0.009	0.640 ± 0.012	11.30	11.71
9107370	4.0583	22.1661	0.42090500	3	0.512 ± 0.009	0.324 ± 0.015	0.322 ± 0.014	0.646 ± 0.021	11.49	11.82
CN And	5.1260	40.2261	0.46279111	4	0.516 ± 0.012	0.277 ± 0.011	0.278 ± 0.014	0.555 ± 0.018	9.70	10.25
6335770	6.3292	32.4657	0.54349740	3	0.377 ± 0.021	0.231 ± 0.006	0.236 ± 0.004	0.467 ± 0.007	10.25	10.56
9093368	6.7958	10.0151	0.52122360	4	0.534 ± 0.013	0.313 ± 0.011	0.299 ± 0.014	0.612 ± 0.018	10.19	10.61
14680632	7.0875	-14.8881	0.40264980	3	0.577 ± 0.017	0.351 ± 0.007	0.351 ± 0.017	0.702 ± 0.018	11.56	11.91
254036	7.1167	78.9619	0.31741200	3	0.586 ± 0.008	0.356 ± 0.015	0.350 ± 0.005	0.706 ± 0.016	10.56	10.93
CL Cet	7.2667	-17.2169	0.62161800	3	0.389 ± 0.007	0.221 ± 0.013	0.233 ± 0.007	0.454 ± 0.015	9.88	10.00
3667194	7.6417	39.4564	0.41711880	3	0.571 ± 0.018	0.337 ± 0.003	0.354 ± 0.002	0.691 ± 0.004	12.08	12.47
9141373	7.6917	14.5461	0.34255000	4	0.589 ± 0.011	0.384 ± 0.017	0.345 ± 0.017	0.729 ± 0.024	11.22	11.55
9124077	8.5542	20.8739	0.34014730	3	0.596 ± 0.008	0.392 ± 0.017	0.368 ± 0.001	0.760 ± 0.017	11.91	12.21

NOTE.—Table 1 is published in its entirety in the electronic edition of the Astronomical Journal. A portion is shown here for guidance regarding its form and content.
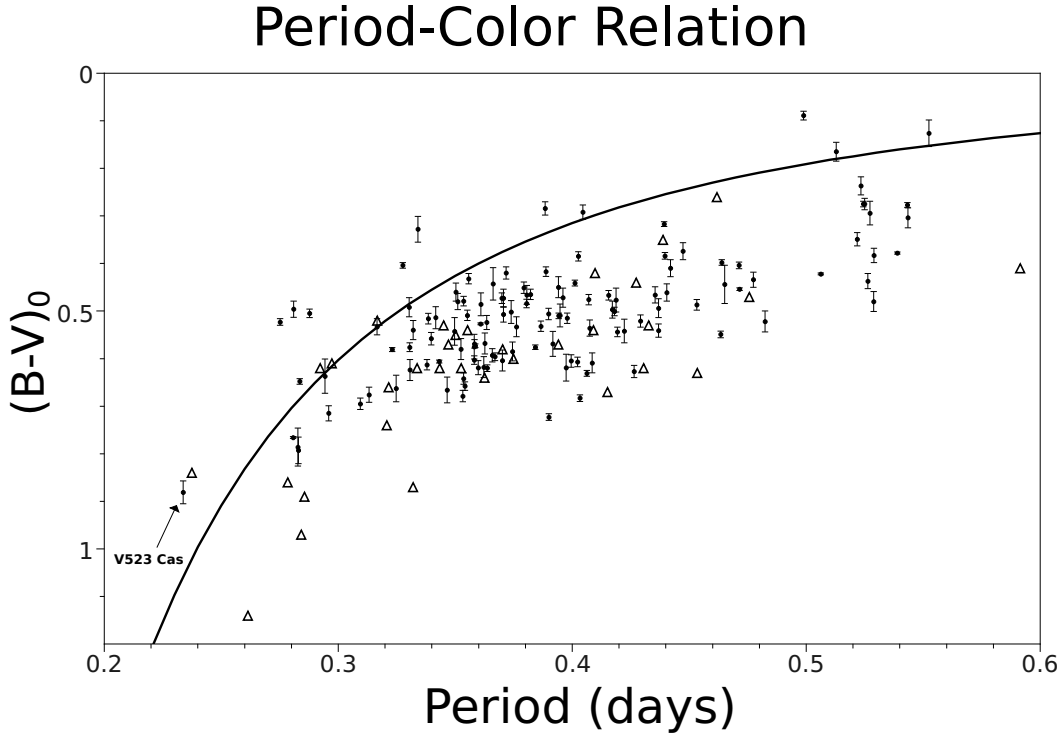

Fig. 6.— Period-color relation for the systems in Table 2 (with error bars) and the systems from Rucinski (1997) with periods less than 0.6 days (triangles). The solid curve is the short period blue envelope (SPBE) from Rucinski (1998). V523 Cas is one of several systems bluer than the SPBE and is discussed in the text.

TABLE 2

REDDENING ESTIMATES FOR THE 101 SYSTEMS SHOWING A MAXIMUM DIFFERENCE OF 0.02 MAG IN $E(B-V)$ BETWEEN THE COLOR DIFFERENCE METHOD AND THE N_{HI} METHOD.

System	$E(B-V)_{CD}$	$E(B-V)_{N_{HI}}$	System	$E(B-V)_{CD}$	$E(B-V)_{N_{HI}}$	System	$E(B-V)_{CD}$	$E(B-V)_{N_{HI}}$
V523 Cas	0.197±0.177	0.191	3091792	0.193±0.042	0.188	GSC 0067-00348	0.110±0.134	0.127
6225358	0.098±0.022	0.087	7209961	0.124±0.042	0.144	14541307	0.085±0.031	0.071
CW Cmi	0.076±0.042	0.077	SX Crv	0.037±0.055	0.054	HO Psc	0.054±0.075	0.054
3962973	0.118±0.064	0.106	5447547	0.090±0.061	0.078	11670840	0.098±0.033	0.087
DF Hya	0.030±0.055	0.047	V1007 Cas	0.184±0.045	0.171	3947987	0.207±0.135	0.199
76033	0.079±0.046	0.081	13007821	0.046±0.042	0.039	4666562	0.097±0.033	0.098
AZ Vir	0.033±0.078	0.025	LZ Dra	0.108±0.082	0.099	15697139	0.041±0.053	0.057
AC Boo	0.039±0.058	0.021	10724466	0.056±0.032	0.065	13120541	0.052±0.046	0.037
14819714	0.064±0.030	0.080	14540910	0.061±0.033	0.071	CK Boo	0.011±0.033	0.025
4701979	0.109±0.051	0.106	QW Gem	0.161±0.064	0.145	V829 Her	0.042±0.025	0.022
VZ Lib	0.090±0.049	0.107	16148635	0.074±0.017	0.085	5269546	0.008±0.042	0.017
V1097 Her	0.052±0.023	0.059	AW CrB	0.019±0.080	0.018	12209034	0.131±0.056	0.144
4750697	0.095±0.049	0.079	7329879	0.052±0.040	0.060	11899139	0.065±0.024	0.058
DZ Psc	0.054±0.130	0.041	GSC 2545-00970	0.000±0.033	0.016	12049671	0.048±0.046	0.044
5261236	0.024±0.057	0.025	XY Boo	0.011±0.043	0.026	14378336	0.070±0.079	0.072
17385764	0.038±0.066	0.028	HV Aqr	0.059±0.064	0.062	7493998	0.037±0.066	0.025
1033806	0.055±0.059	0.041	LO And	0.140±0.031	0.155	11370982	0.110±0.079	0.130
7269084	0.086±0.056	0.093	BI CVn	0.017±0.021	0.018	10142767	0.041±0.030	0.054
5214166	0.041±0.036	0.026	V1036 Her	0.069±0.061	0.059	7336416	0.068±0.092	0.065
17357108	0.048±0.021	0.047	609692	0.131±0.095	0.137	2643685	0.013±0.063	0.027
AR CrB	0.043±0.069	0.050	908512	0.070±0.046	0.084	9221283	0.074±0.033	0.067
BL Dra	0.083±0.079	0.073	14591442	0.051±0.032	0.048	6099330	0.178±0.089	0.172
10476945	0.008±0.022	0.026	2888729	0.041±0.046	0.035	4805949	0.048±0.060	0.056
2657877	0.024±0.035	0.021	3667194	0.074±0.045	0.075	15779695	0.079±0.081	0.091
10608583	0.053±0.038	0.055	4873888	0.038±0.059	0.020	4760150	0.072±0.059	0.059
2795010	0.023±0.048	0.023	13259318	0.042±0.059	0.028	13363862	0.032±0.033	0.050
XY LMi	0.021±0.060	0.021	ET Psc	0.057±0.040	0.061	6375021	0.078±0.046	0.079
16134469	0.074±0.094	0.093	11905222	0.041±0.023	0.046	9311873	0.241±0.041	0.228
15595338	0.057±0.142	0.057	V728 Her	0.006±0.046	0.024	14560232	0.059±0.069	0.071
V2759 Ori	0.254±0.047	0.261	10141474	0.054±0.042	0.056	14304024	0.084±0.104	0.097
1206915	0.102±0.076	0.101	1033721	0.057±0.093	0.039	3791537	0.101±0.052	0.116
RU UMi	0.037±0.062	0.019	V843 Mon	0.241±0.083	0.224	BC Eri	0.053±0.130	0.072
TZ Lyr	0.043±0.066	0.052	ES UMa	0.056±0.079	0.073	14678045	0.047±0.052	0.044
6335770	0.073±0.093	0.070	2962451	0.040±0.127	0.043			

Bradstreet, D.H. 1985, ApJS, 58, 413

Cardelli, J.A., Clayton, G.C. & Mathis, J.S. 1989, ApJ, 345, 245

Cousins, A.W.J. 1978, MNASSA, 37, 62

Droege, T.F., Richmond, M.W., Sallman, M.P. & Creager, R.P. 2006, PASP, 118, 1666

Eggen, O. J. 1967, Mem. Royal Ast. Soc., 70, 111

Getel, S.J., Geske, M.T. & McKay, T.A. 2006, AJ, 131, 621

Hilditch, R.W. & Bell, S.A. 1987, MNRAS, 229, 529

Hrivnak, B.J. 1985, ApJ, 290, 696

Johnson, H.L. & Morgan, W.W. 1953, ApJ, 117, 313

Lucy, L. B. 1968, ApJ, 151, 1123

Munari, U., & Zwitter, T. 1997, A&A, 318, 269

Nelson, C.A. & Eggleton, P.P. 2001, ApJ, 552, 664

Predehl, P. & Schmitt, J.H.M.M. 1995, A&A, 293, 889

Pribulla, T., Kreiner, J.M. & Tremko, J. 2003, Multiple Stars Across the H-R Diagram, ESO Astrophysics Symposia, 33, 38

Pribulla, T. & Rucinski, S.M. 2008, Contr. of the Astron. Observatory Skalnate Pleso, 2008, 163

Rucinski, S.M. 1997a, Inf. Bull. Variable Stars, No. 4460

Rucinski, S.M. 1997b, PASP, 109, 1340

Rucinski, S.M. 1998, AJ, 116, 2998

Rucinski, S.M. 2006, MNRAS, 368, 1319

Samec, R.G., Faulkner, D.R., & Williams, D.B. 2004, AJ, 128, 2997

Stępień, K. 2009, MNRAS, 397, 857

Stępień, K. 2011, Acta Astron., 126, 2988

Terrell, D., Munari, U., Zwitter, T., & Nelson, R.H. 2003, AJ, 126, 2988

Walker, A.R. 1985, MNRAS, 213, 889

Wilson, R.E. 2001, Inf. Bull. Variable Stars, No. 5076